



Vapor-Induced Motion of Two Pure Liquid Droplets

Journal:	<i>Soft Matter</i>
Manuscript ID	SM-COM-12-2018-002584.R1
Article Type:	Communication
Date Submitted by the Author:	15-Jan-2019
Complete List of Authors:	<p>Wen, Yanqing; Beijing University of Chemical Technology Kim, Paul; University of Massachusetts Amherst, Polymer Science and Engineering Shi, Shaowei; Beijing University of Chemical Technology, College of Materials Science and Engineering Wang, Dong; State Key Laboratory of Organic-inorganic Composites, Beijing University of Chemical Technology Man, Xingkun; Beihang University, Physics department, BUAA Doi, Masao; Beihang University, Center of Soft Matter Physics and its Applications Russell, Thomas; University of Massachusetts, Polymer Science and Engineering Department</p>



Vapor-Induced Motion of Two Pure Liquid Droplets

Yanqing Wen^a, Paul Y. Kim^b, Shaowei Shi^{*a}, Dong Wang^c, Xingkun Man^{*d}, Masao Doi^d, and Thomas P. Russell^{*a,b,e,f}

Received 00th January 20xx,
Accepted 00th January 20xx

DOI: 10.1039/x0xx00000x

www.rsc.org/

The movement of evaporating liquid droplets on a surface can be triggered by the Marangoni effect arising from heterogeneities in the surface tension or a gradient in the surface energy of the substrate. Here, we show that, on a high energy surface that remains uniform, the motion of two pure liquid droplets can be induced by a gradient in the liquid vapor resulting from evaporation. The droplets always attract each other, moving from the high evaporation side to the low evaporation side, to reduce energy dissipation. By varying the volume of the droplets or the distance between droplets, the motion of the droplets can be effectively controlled.

Inducing and controlling the movement of droplets in a prescribed manner on a solid substrate has important ramifications for technical applications, ranging from coatings to microfluidics to heat transfer devices, but also can aid in our understanding of phenomena observed in nature where the motion of water droplets, for example, is critical for survival. Usually droplet motion can be achieved by an imbalance in the interfacial tension of the droplet with the substrate and the surface energies of the droplet and the substrate. This can be produced by gradients in temperature¹⁻³ or composition^{4,5} of a liquid surface, which is the well-known Marangoni effect,⁶ for example the “tears of wine” phenomenon observed in a wine

glass. Variations in the surface tension of a solid substrate, e.g. a surface with a gradient in the surface energy⁷ or wettability,⁸⁻¹⁴ that give rise to a hysteresis in the contact angle, can also induce such a directed motion. Here, liquid droplets that have a surface energy lower than that of the substrate, will move towards the area with higher surface energy to reduce the free energy of the system. Much experimental and theoretical attention has been given to these two mechanisms and various strategies to manipulate surface wettability and the motion of droplets, as seen with light-driven motion⁷ and the fast motion of liquid droplets^{10,11} have been realized.

Recently, by using mixtures of two miscible liquids, specifically propylene glycol (PG) and water, Cira et al found that, on a high energy substrate where the wettability is uniform and unchanged, the mixtures do not spread but rather form stable droplets, which is explained by an evaporation-induced Marangoni effect.⁵ They also demonstrated that these droplets can move in response to the vapor emitted by neighboring droplets and fascinating droplet motion, including attraction, repulsion and “chasing” can be achieved. The increased vapor concentration between the droplets leads to less evaporation, causing an inhomogeneous local surface tension. Such a nonuniformity in the surface tension causes a Marangoni flow, leading to the droplet motion. Based on this study, the question arises as to the behavior of two droplets of same pure liquid and whether the motion of the droplets can be induced and, if so, what is the mechanism inducing the motion? Here, the mechanism described by Cira et al is not applicable, since there should be no Marangoni effect.⁵

Using the Onsager principle, Man et al theoretically predicted the motion of two pure liquid droplets on an inert substrate and proposed a new mechanism for the droplet motion.¹⁵⁻¹⁹ They showed that, even in the absence of the Marangoni effect, droplet motion can be induced by a gradient in the evaporation rate of the droplets.²⁰⁻²⁷ The non-uniform evaporation rate drives droplet move from the high evaporation side to low evaporation side to reduce the energy dissipation associated with the inherent fluid flow induced by evaporation. Here, we

^a Beijing Advanced Innovation Center for Soft Matter Science and Engineering, Beijing University of Chemical Technology, Beijing 100029, China.
E-mail: shisw@mail.buct.edu.cn; russell@mail.pse.umass.edu

^b Polymer Science and Engineering Department, University of Massachusetts, Amherst, Massachusetts 01003, USA.

^c State Key Laboratory of Organic-Inorganic Composites, Beijing University of Chemical Technology, Beijing 100029, China.

^d Center of Soft Matter Physics and Its Applications & School of Physics and Nuclear Energy Engineering, Beihang University, Beijing 100191, China.
E-mail: manxk@buaa.edu.cn

^e Materials Sciences Division, Lawrence Berkeley National Laboratory, 1 Cyclotron Road, Berkeley, California 94720, USA.

^f Advanced Institute of Materials Research (AIMR), Tohoku University, 2-1-1 Katahira, Aoba, Sendai 980-8577, Japan.

† Footnotes relating to the title and/or authors should appear here.

Electronic Supplementary Information (ESI) available: [details of any supplementary information available should be included here]. See DOI: 10.1039/x0xx00000x

experimentally prove this mechanism and realize effective control of droplet motion.

High energy substrates were achieved by cleaning glass microscope slides in a 7:3 (v/v) mixture of concentrated sulfuric acid and 30% hydrogen peroxide (piranha solution). After removal from the acid bath, the substrates were thoroughly washed in de-ionized water and then dried under a nitrogen gas flow. The substrates were used immediately after cleaning or stored in an inert atmosphere until use. All experiments were performed in a controlled humidity chamber at room temperature. *n*-hexane is used as the model droplet in this study, due to its vapor pressure (150.9 ± 0.1 mmHg at 25°C , $\gamma_{LV} = 17.9$ mN/m) and, importantly, it can form stable droplets on a high energy substrate with a contact angle of 6.5° , consequently the curvature of the droplets is very low. This conforms to the conditions used in the theoretical model with $R \gg H$, where R and H are the radius and height of the droplet. PG and water are not suitable candidates because they spread completely when deposited on the substrate, where the spreading parameter $S = \gamma_{SV} - (\gamma_{LV} + \gamma_{SL}) > 0$, here γ_{SV} , γ_{LV} , and γ_{SL} are the interfacial tensions between solid/vapor, liquid/vapor, and solid/liquid (Video S1). In this case, no gradient in the evaporation rate is formed across the droplets and, as a result, no droplet motion is observed.

Figure 1 and Video S2 show the motions of two $5 \mu\text{L}$ *n*-hexane droplets on the substrate with homogenous surface energy. No movement was observed when a single droplet is placed on the substrate. However, in the presence of another droplet of the same liquid in close proximity (< 3 mm apart), by a long-range interaction, the two droplets move toward each other, induced by the evaporation of the *n*-hexane, and then coalescence into one droplet. In addition to *n*-hexane, we also found liquids, such as cyclohexane (97.6 mmHg at 25°C , $\gamma_{LV} = 24.7$ mN/m) and ethyl acetate (94.7 mmHg at 25°C , $\gamma_{LV} = 29.2$ mN/m), that formed stable droplets and attracted each other (Video S3). This result provides experimental evidence that vapor gradients from solvent evaporation can induce the motion of pure droplets. For the case presented, each droplet lies in the vapor gradient produced by the other, causing a local increase in the vapor concentration and, therefore, a decrease in the evaporation on the adjacent portions of the droplets, breaking evaporation symmetry. The non-uniform evaporation rate moves the droplet from the high evaporation side to the low evaporation side, which can be understood by the minimum energy dissipation principle in Stokes hydrodynamics.¹⁹

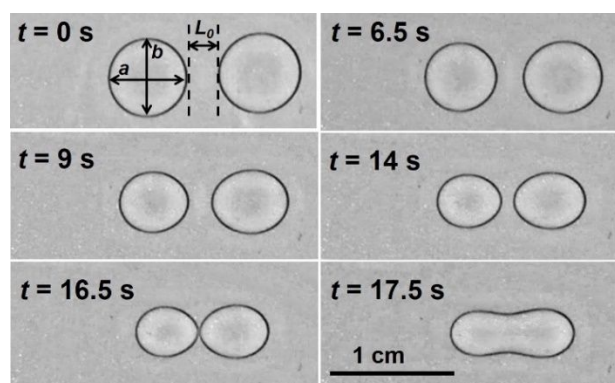


Fig. 1 The motion behavior of two $5 \mu\text{L}$ *n*-hexane droplets on a high energy substrate. These two droplets are deposited from left to right in a short time, with an initial shortest edge-to-edge distance L_0 of ~ 2.7 mm.

To further support this argument, we passed a uniform, gentle flow of nitrogen onto the droplets to remove or significantly reduce the vapor gradient between the droplets and found that the motion could be completely arrested. When the nitrogen flow was stopped, the two droplets again moved toward each other due to the recovered vapor gradient (Video S4). Also, this vapor-induced motion of two pure liquid droplets can be realized when there is a physical break in the substrate between the droplets. Here, two glass slides were used and were placed next to one another, but not touching, and droplets of *n*-hexane were placed on each (Video S5). As in the continuous substrate case, the droplets moved toward each other, then stopped at the edge of the substrates, clearly showing that droplet motion is not due to a thin, wetting-layer film between the two droplets. Furthermore, we showed two droplets approaching each other even on two glass slides with slight height difference (0.13 - 0.17 mm, Video S6).

We also observed a deformation of the droplet during the motion process where the droplets shape changed from the initial circular shapes to an egg-like shape pointed toward each other. In the analysis we assume the shape to be elliptical with a major (long) and minor (short) axis. To quantify the motion behavior of the droplets, including the velocity and the deformation, a custom-made Matlab code was used. By plotting L/L_0 as a function of $\tau - t$, where L is the shortest edge-to-edge distance between droplets, L_0 is the initial shortest edge-to-edge distance between droplets (~ 2.7 mm), and τ is the time of droplet contact, we observed that the speed of two droplets increased as they approached each other. Our theoretical model shows that the velocity of the droplet induced by the gradient of evaporation rate is,¹⁹

$$\frac{dx_c(t)}{dt} = -\frac{R}{\theta} \beta_j \quad (1)$$

where, $x_c(t)$ is the center of the droplet contact line, θ is the apparent contact angle, and β_j is a constant parameter to describe the gradient of the evaporation rate. Equation (1) is solved using the full expansions of $R(t)$, $V(t)$ and $\theta(t)$. All variables are time dependent, so:

$$\tau_{ev} \frac{dR(t)}{dt} = -\frac{V_0 R^2}{4R_0 V} + \frac{V_0^{\frac{1}{3}}}{6CK_{ev}\theta_e^2} \theta(\theta^2 - \theta_e^2) \quad (2)$$

$$\tau_{ev} \frac{dV(t)}{dt} = -\frac{V_0}{R_0} R \quad (3)$$

$$\theta(t) = \frac{4V}{\pi R^3} \quad (4)$$

where V_0 and R_0 are the initial droplet volume and contact line radius, θ_e is the equilibrium contact angle, τ_{ev} is the characteristic time for the droplet to fully evaporate, and C is a constant. This full model has two fitting parameters K_{ev} (the evaporation rate) and β_j . As the two droplets are initially separated by a distance that is smaller than the droplet size in the experiments, we assume that both parameters are constant during the evaporation. Using the assumption, we can calculate the shape evolution and the center velocity of the droplet for given K_{ev} and β_j . We set the value of these parameters by fitting the result with experimental data. Then, we calculated the edge-to-edge distance $L(t)$ via $L(t) = L_0 - \dot{x}t$. The comparison between theoretical and experimental results of L/L_0 as a function of $\tau - t$ is shown in Figure 2a, which shows that good agreement was obtained.

By plotting a/b as a function of $\tau - t$, where a and b are the long and the short axes of the droplet, respectively, we observed that the degree of deformation also increased as the two droplets approached each other (Figure 2b). The droplet deformation arises mainly from the contact angle hysteresis.²⁸⁻³¹ To move, the contact angle at the moving front must be larger than the advanced contact angle θ_A , while it has to be smaller than the receding contact angle θ_R on the other side. The asymmetry between $\theta_A - \theta_e$ and $\theta_e - \theta_R$ leads to different moving velocities for the advancing and receding contact lines, respectively, causing the droplet deformation. It should be noted that the theoretical model is for an ideal situation without contact angle hysteresis.¹⁹

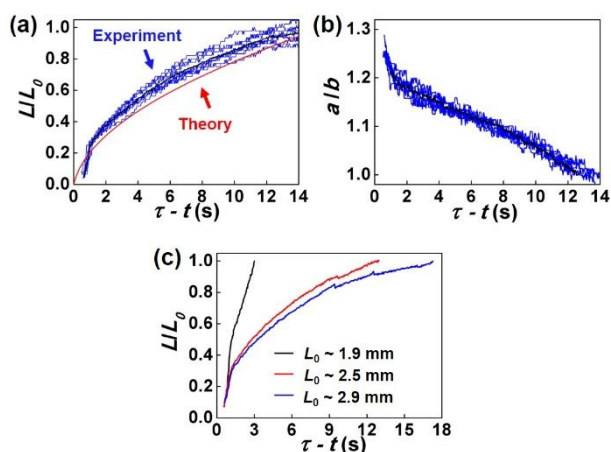


Fig. 2 Velocity and deformation for two freely moving 5 μL n -hexane droplets. (a) Normalized distance L/L_0 between two droplets as a function of $\tau - t$ ($L_0 \sim 2.7$ mm; blue curve: experimental result; black curve: average experimental result; red curve: theoretical result). (b) The degree of deformation (a/b) of the left droplet as a function of $\tau - t$. (c) Normalized

distance L/L_0 between two droplets as a function of $\tau - t$ with different L_0 .

Further support of the evaporation-induced droplet motion is found when two droplets were sequentially deposited onto the substrate surface, the second droplet that was deposited (termed as D_2) always moved initially and moved a longer distance than the droplet deposited initially (termed as D_1). When D_1 is placed on the substrate, the uniform evaporation rate produces a vapor gradient around the droplet. When D_2 is deposited close to D_1 , the pre-existing vapor gradient of D_1 will immediately influence the evaporation rate of D_2 , giving rise to a non-uniform evaporation rate across the droplet, driving the movement of D_2 toward D_1 . As D_2 evaporates and approaches, the gradient of vapor produced by D_2 will in turn affect the evaporation of D_1 , inducing a hysteretic motion of D_1 toward D_2 . If the distance between D_1 and D_2 is too large (> 3 mm), the effect of the vapor gradient of D_1 on D_2 is significantly weakened and no movement of the droplets is observed. Within a critical distance (termed the longest distance that droplets can move), we found that the velocity of the droplets decreased (a reduction in slope) as the distance between the droplets increased (Figure 2c). This is understandable because, at a greater distance, the heterogeneity in the evaporation rate across the droplets is smaller, releasing a weak vapor signal to droplets, leading to reduced motion.

We further investigated the motion of large-small droplet pairs with L_0 of ~ 2.7 mm. The volume of the larger droplet (deposited initially) varies from 5 μL to 60 μL , while the volume of the smaller droplet (deposited secondly) is kept constant at 1 μL . Unlike the results of two droplets with the same volume, for the large-small pair, the larger droplet did not move, while the smaller droplet always moved toward the larger droplet (Video S7). The larger droplet provides a stronger vapor gradient environment than the smaller one and has a greater effect on the evaporation rate of the smaller droplet. The vapor gradient produced by the small droplet is weak and, in comparison, can even be ignored, if the volume difference between the droplets is sufficiently large. Also, it is possible that contact angle hysteresis plays a role here in inhibiting the large droplet from moving. In the presence of contact angle hysteresis, the threshold force to activate the droplet motion increases with the length of contact line. For a large droplet, this threshold cannot be met by the capillary force induced by the vapor gradient produced by the small droplet. By varying the volume of the larger droplet, the velocity of the smaller droplet can be tuned. As shown in Figure 3a, we observed that the greater the volume of the larger droplet, the faster is the velocity of the smaller droplet motion, which can also be explained by the degree of the heterogeneity in the evaporation rate across the small droplet. The deformation of the smaller droplet is shown in Figure 3b, which shows that the higher the velocity of the droplet, the greater is the deformation during the motion process (Video S7).

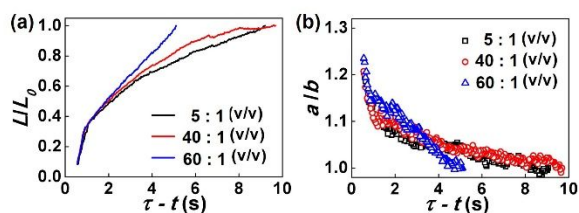


Fig. 3 Velocity comparison of a big-small droplet pair and the deformation of small droplet. (a) Normalized distance L/L_0 between two droplets as a function of $\tau - t$. (b) The degree of deformation a/b of the left droplet as a function of $\tau - t$.

As we discussed above, for the droplet pair with equal droplet volumes, the droplet deposited second always moves initially, followed by the movement of the droplet deposited initially. For the large-small droplet pair with relatively large volume differences, the smaller droplet that is deposited secondly moves toward the larger droplet, while the larger droplet does not move. However, for the large-small droplet pair, if we change the deposition order of the droplets and deposit the smaller droplet first, will the larger droplet in response to the gradient established by the initial smaller droplet? Figure 4 shows a comparison using two droplets, the larger with a volume of $5 \mu\text{L}$ and the smaller with a volume of $1 \mu\text{L}$. It is evident that the larger droplet can move toward the smaller droplet, but the smaller droplet moves also. It was difficult to determine which droplet moves initially. In repeated experiments, three results were observed (the smaller droplet moves initially, the larger droplet moves initially, and both droplets move simultaneously). These results show that there is a delicate balance between the existing vapor gradient from the smaller droplet and subsequently produced vapor gradient from the larger droplet, and the motion order of the two droplets is a result of the interaction between these two vapor gradients, which was difficult to control under the experimental conditions, since the placement of the second larger droplet takes a finite amount of time to complete. Similar results were observed when using larger droplets with even greater volumes (Video S8).

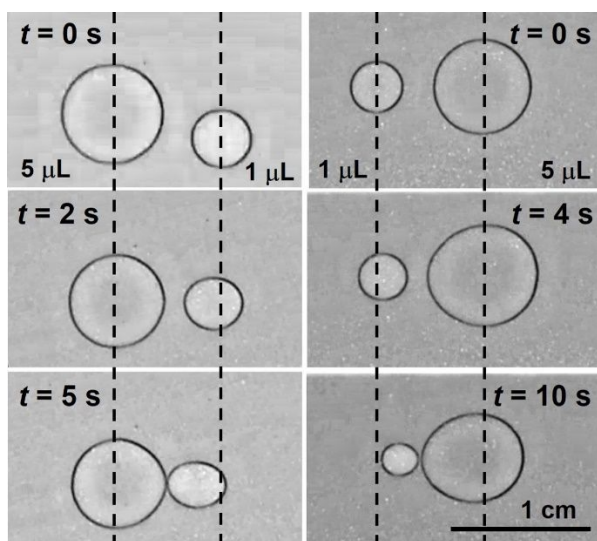


Fig. 4 Motions of large-small droplet pair by changing the deposition order of droplets. The vertical dashed lines are the initial positions of the centers of the droplets (left: the big droplet was deposited first; right: the small droplet was deposited first).

Conclusions

In summary, we show proof for a new droplet motion mechanism where the gradient of evaporation rate can induce the motion of droplets from the high evaporation side to the low evaporation side. The experimental data of the motion of two identical pure liquid droplets is in good agreement with theoretical predictions. The vapor gradient produced by one droplet plays an important role in controlling the evaporation rate of a second droplet, resulting in a movement of the droplets toward each other. The movement can be induced, stopped, and accelerated by tuning parameters such as the volume of the droplets and the separation distance between the droplets.

The mechanism of the droplet motion we proposed in this paper is based on our macroscopic observations. The droplet motion may be affected by the local structures, such as a precursor film that may form around droplets. If the film has a gradient in surface tension or disjoining pressures due to the gradient in the vapor density, it may generate a force to drive droplet motion. However, the effects of the asymmetric vapor density on the surface tension and the disjoining pressure are not known. A preliminary consideration, assuming that the surface tension and the disjoining pressure (i.e., the inverse of the film thickness) decreases with an increase of the vapor density, indicates that the two droplets will move away from rather than approach each other. We therefore stayed within our macroscopic model and left this issue for future studies. Understanding the mechanism underpinning such motion will be of great interest coatings, microfluidics and self-cleaning surfaces.

Conflicts of interest

There are no conflicts to declare.

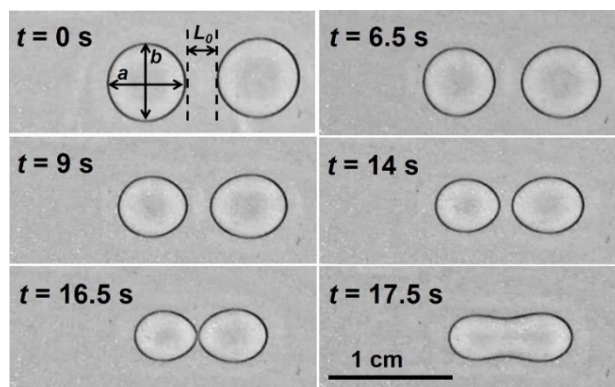
Acknowledgements

This work was supported by Grants NO. 2194083 of Beijing Natural Science Foundation, Grants No. 21822302 and No. 21434001 of the National Natural Science Foundation of China (NSFC), and the NSFC-ISF Research Program, jointly funded by the NSFC under Grant No. 51561145002 and the Israel Science Foundation (ISF) under Grant No. 885/15. PYK and TPR were supported by the Army Research Office under contract W911NF-17-1-0003. We also thank the useful comments of the reviewer.

References

- 1 F. Brochard, *Langmuir*, 1989, **5**, 432.

- 2 J. B. Brzoska, F. B. Wyart, F. Rondelez, *Langmuir*, 1993, **9**, 2220.
- 3 M. K. Chaudhury, A. Chakrabarti, T. Tibrewal, *Extreme Mech. Lett.*, 2014, **1**, 104.
- 4 R. L. Cottingham, C. M. Murphy, C. R. Singleterry, *Adv. Chem. Ser.*, 1946, **43**, 341.
- 5 N. J. Cira, A. Benusiglio, M. Prakash, *Nature*, 2015, **519**, 446.
- 6 J. Thomson, *Phil. Mag. Ser. 4*, 1855, **10**, 330.
- 7 K. Ichimura, S. Oh, M. Nakagawa, *Science*, 2000, **288**, 1624.
- 8 M. K. Chaudhury, G. M. Whitesides, *Science*, 1992, **256**, 1539.
- 9 F. D. Dos Santos, T. Ondarcuhu, *Phys. Rev. Lett.*, 1995, **75**, 2972.
- 10 S. Daniel, M. K. Chaudhury, J. C. Chen, *Science*, 2001, **291**, 633.
- 11 D. T. Wasan, A. D. Nikolov, H. Brenner, *Science*, 2001, **291**, 605.
- 12 R. J. Petrie, T. Bailey, C. B. Gorman, J. Genzer, *Langmuir*, 2004, **20**, 9893.
- 13 C. Sun, X. W. Zhao, Y. H. Han, Z. Z. Gu, *Thin Solid Films*, 2008, **516**, 4059.
- 14 B. Chandesris, U. Soupremanien, N. Dunoyer, *Colloids and Surfaces A: Physicochem. Eng. Aspects*, 2013, **434**, 126.
- 15 M. Doi, *Chin. Phys. B*, 2015, **24**, 020505.
- 16 X. M. Xu, Y. Di, M. Doi, *Phys. Fluids*, 2016, **28**, 087101.
- 17 X. K. Man, M. Doi, *Phys. Rev. Lett.*, 2016, **116**, 066101.
- 18 S. Hu, Y. Wang, X. Man, M. Doi, *Langmuir*, 2017, **33**, 5965.
- 19 X. K. Man, M. Doi, *Phys. Rev. Lett.*, 2017, **119**, 044502.
- 20 R. D. Deegan, O. Bakajin, T. F. Dupont, G. Huber, S. R. Nagel, T. A. Witten, *Nature*, 1997, **389**, 827.
- 21 R. D. Deegan, O. Bakajin, T. F. Dupont, G. Huber, S. R. Nagel, T. A. Witten, *Phys. Rev. E*, 2000, **62**, 756.
- 22 C. Schäfle, C. Bechinger, B. Rinn, C. David, P. Leiderer, *Phys. Rev. Lett.*, 1999, **83**, 5302.
- 23 M. Cachile, O. Bénichou, C. Poulard, A. M. Cazabat, *Langmuir*, 2002, **18**, 7985.
- 24 M. Cachile, O. Bénichou, C. Poulard, A. M. Cazabat, *Langmuir*, 2002, **18**, 8070.
- 25 H. Hu, R. G. Larson, *J. Phys. Chem. B*, 2002, **106**, 1334.
- 26 R. G. Picknett, R. Bexon, *J. Colloid Interface Sci.*, 1977, **61**, 336.
- 27 O. Carrier, N. S. Bonn, R. Zargar, M. Aytouna, M. Habibi, J. Eggers, D. Bonn, *J. Fluid Mech.*, 2016, **798**, 774.
- 28 R. H. Dettre, R. E. Johnson, *Adv. in Chem. Ser.*, 1964, **43**, 136.
- 29 B. He, J. Lee, N. A. Patankar, *Colloids and Surfaces A: Physicochem. Eng. Aspects*, 2004, **248**, 101.
- 30 D. Bonn, J. Eggers, J. Indekeu, J. Meunier and E. Rolley, *Rev. Mod. Phys.*, 2009, **81**, 739.
- 31 R. D. Deegan, *Phys. Rev. E*, 2000, **61**, 475.



Vapor-Induced Motion of Two Pure Liquid Droplets